

SCIENTIFIC REPORTS

OPEN

Inversions and adaptation to the plant toxin ouabain shape DNA sequence variation within and between chromosomal inversions of *Drosophila subobscura*.

Received: 09 November 2015

Accepted: 14 March 2016

Published: 31 March 2016

Cinta Pegueroles^{1,2,3}, Albert Ferrés-Coy⁴, Maria Martí-Solano⁵, Charles F Aquadro⁶, Marta Pascual¹ & Francesc Mestres¹

Adaptation is defined as an evolutionary process allowing organisms to succeed in certain habitats or conditions. Chromosomal inversions have the potential to be key in the adaptation processes, since they can contribute to the maintenance of favoured combinations of adaptive alleles through reduced recombination between individuals carrying different inversions. We have analysed six genes (*Pif1A*, *Abi*, *Sqd*, *Yrt*, *Atpα* and *Fmr1*), located inside and outside three inversions of the O chromosome in European populations of *Drosophila subobscura*. Genetic differentiation was significant between inversions despite extensive recombination inside inverted regions, irrespective of gene distance to the inversion breakpoints. Surprisingly, the highest level of genetic differentiation between arrangements was found for the *Atpα* gene, which is located outside the O₁ and O₇ inversions. Two derived unrelated arrangements (O₃₊₄₊₁ and O₃₊₄₊₇) are nearly fixed for several amino acid substitutions at the *Atpα* gene that have been described to confer resistance in other species to the cardenolide ouabain, a plant toxin capable of blocking ATPases. Similarities in the *Atpα* variants, conferring ouabain resistance in both arrangements, may be the result of convergent substitution and be favoured in response to selective pressures presumably related to the presence of plants containing ouabain in the geographic locations where both inversions are present.

Adaptation is a major evolutionary mechanism that allows organisms to live in certain habitats or conditions^{1,2}. Prime evidence for adaptation is the maintenance and reproducibility of latitudinal clines in the frequency of chromosomal inversions observed in continuous populations of several species of drosophilids across continents³⁻⁶. In particular, *Drosophila subobscura* has been studied extensively due to its abundant inversion polymorphism and its recent invasion of large areas of North and South America. The frequencies of most chromosomal inversions in *D. subobscura* are correlated with latitude in the Palearctic region. In addition, similar latitudinal clines were also detected in both colonized American regions, suggesting that the geographic distribution of its inversion polymorphism is adaptive and not a mere consequence of historic events^{3,7,8}. The chromosomal arrangements of *D. subobscura* are formed by single and overlapped inversions that may differentially affect levels of nucleotide variability, since the overlapped inversions may effectively reduce recombination. Previous studies focused on chromosomal inversions located in the segment I of the O chromosome (Fig. 1) and the A

¹Departament de Genètica and IRBio, Facultat de Biologia, Universitat de Barcelona, Barcelona 08028, Spain.

²Centre for Genomic Regulation (CRG), The Barcelona Institute of Science and Technology, Dr. Aiguader 88, Barcelona 08003, Spain.

³Universitat Pompeu Fabra (UPF), Barcelona, Spain.

⁴Department of Neurochemistry and Neuropharmacology, IIBB-CSIC, Barcelona, Spain.

⁵Research Programme on Biomedical Informatics (GRIB), Department of Experimental and Health Sciences, Universitat Pompeu Fabra, IMIM (Hospital del Mar Medical Research Institute), Dr. Aiguader, 88, 08003 Barcelona, Spain.

⁶Department of Molecular Biology and Genetics, Cornell University, Ithaca, New York 14853, USA.

Correspondence and requests for materials should be addressed to C.P. (email: cintapq@gmail.com)

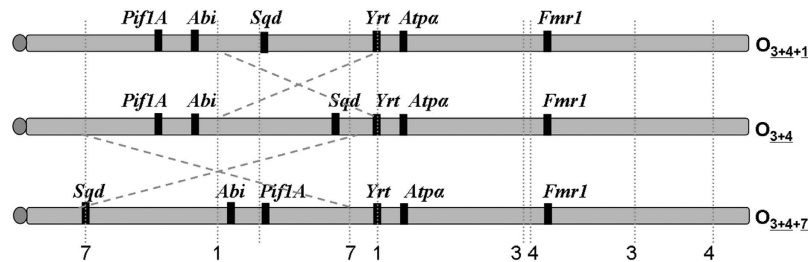


Figure 1. Chromosomal location for the six gene regions studied (*Pif1A*, *Abi*, *Sqd*, *Yrt*, *Atpα* and *Fmr1*) in O_{3+4} , O_{3+4+1} and O_{3+4+7} arrangements. Dashed lines indicate the location of the O_1 and O_7 inversion.

chromosome^{9–13}, but segment II of the O chromosome remains largely unexplored despite bearing some chromosomal inversions whose frequencies cycle seasonally and respond to acute environmental events¹⁴.

The three chromosomal arrangements analysed in the present study (O_{3+4} , O_{3+4+1} and O_{3+4+7}) differ by the presence of single chromosomal inversions in the segment II of the O chromosome (Fig. 1). They can be considered medium size inversions since O_1 includes 6.09 Mb and O_7 inversion 11.76 Mb (estimated as in Pegueroles *et al.*¹⁵). The three arrangements are negatively correlated with latitude in the Palearctic region¹⁶, and one of them (O_{3+4+7}) shows seasonal fluctuations¹⁷. These arrangements are found in sympatry in some regions around the Mediterranean Sea, although with different abundances⁸. The samples for the present research are from two well-studied localities, Barcelona and Mt. Parnes, where these arrangements coexist¹⁸.

Our aim is to test whether selection or drift are the evolutionary forces shaping genetic variability in single medium-size chromosomal inversions. We inferred population recombination and analysed patterns of DNA variation and linkage disequilibrium in six gene segments located within inverted and non-inverted regions, taking into account the age, the length of the inverted regions and the distance to the inversion breakpoint. We also evaluated whether variability patterns fit selectively neutral expectations using both evolutionary and protein structural approaches. We found significant genetic differentiation between arrangements despite extensive recombination being detected inside the inversions. Interestingly, we found nonsynonymous substitutions at the *Atpα* gene outside the inverted regions that appear to have been fixed by positive selection in association with both the O_{3+4+1} and O_{3+4+7} arrangements, and that occur at residues in the structure of the ATPase α subunit which are known to confer resistance to the plant toxin ouabain.

Results

Nucleotide variation and genetic differentiation. To characterize the genetic content of the O_{3+4+1} and the O_{3+4+7} arrangements, we first calculated nucleotide variation and divergence for each of the six gene fragments studied (Table 1). Sequences for O_{3+4} individuals are from Pegueroles *et al.*¹¹ and diversity estimates are reported herein to facilitate comparison. The number of haplotypes was approximately the same as the number of analysed lines, except for *Sqd* and *Atpα* genes in O_{3+4+1} arrangement that had lower numbers of haplotypes (Table 1). Considering the variability of the O_{3+4} arrangement as a baseline, we observed a decrease in variability in the intronic regions of *Sqd* and *Atpα* genes at both inverted arrangements (Fig. 2). In contrast, we observed increased variability in the first exonic region of *Atpα* gene for the O_{3+4+7} arrangement. Diversity levels were highly variable between genes (Table 1, Fig. 2). The intronic regions of the *Pif1A* gene showed the highest diversity (π) for all three arrangements despite being located within the O_7 inversion. The *Yrt* gene also showed high π levels despite most of the amplified fragment being exonic and located close to the O_1 breakpoint and outside the inversion. Since the proportion of intronic-exonic regions amplified varied among genes, genetic variability was also estimated in silent positions exclusively (i.e., both synonymous and non-coding sites) to avoid biases in diversity estimates (Table 1). In agreement with π results, silent nucleotide variability (π_{sil}) remained highly variable among genes, but quite similar when comparing the two inverted arrangements. No relationship was detected between π and distance to breakpoints, since Pearson correlation values were negative and non-significant for all arrangements.

Most genes located inside the inverted regions showed significant genetic differentiation between arrangements (Table 2). However, the largest significant F_{ST} values were found for the *Atpα* gene, which is located close to but outside the studied inversions. Since recombination is expected to be constrained near inversion breakpoints, we plotted genetic differentiation with respect to the distance to nearest breakpoint. No relationship between genetic differentiation and distance to the nearest inversion breakpoint was found (Pearson correlation values were negative and non-significant) with most of the genes having similar F_{ST} values regardless of their location within or outside the inverted region (Suppl. Fig. 1).

Linkage disequilibrium, gene flux and age of the inversions. If chromosomal inversions are effectively reducing recombination levels, we would expect higher levels of LD within and between genes located inside them. However, levels of LD in these genes were very low and only a strong LD was observed within the *Atpα* gene (Fig. 3A). Significant associations after adjusting for multiple testing (in green) were obtained only within genes and never between genes regardless of their location in relation to the inversions (Fig. 3B–D). The highest ZnS values were obtained for the *Atpα* gene with 0.34 and 0.26 when analyzing together inversions O_{3+4} – O_{3+4+1} and O_{3+4} – O_{3+4+7} , respectively (Table S1). Surprisingly, ZnS values were in general higher for O_{3+4+1}

Gene	Pop	Arrangement	<i>n</i>	<i>h</i>	<i>S</i>	Singletons	π	π_{sil}	θ_{sil}	K_{sil}
<i>Pif1A</i>	MP	O_{3+4+1}	9	9	104	61	0.021	0.022	0.025	0.188
		O_{3+4}	12	12	120	55	0.021	0.023	0.026	0.191
	BC	O_{3+4+7}	9	9	89	54	0.017	0.018	0.021	0.187
		O_{3+4}	12	12	114	42	0.022	0.023	0.024	0.190
<i>Abi</i>	MP	O_{3+4+1}	3	3	8	8	0.003	0.008	0.008	0.174
		O_{3+4}	12	12	32	20	0.005	0.012	0.017	0.173
	BC	O_{3+4+7}	10	9	33	21	0.006	0.015	0.018	0.172
		O_{3+4}	7	7	24	15	0.006	0.014	0.015	0.173
<i>Sqd</i>	MP	O_{3+4+1}	10	5	12	8	0.002	0.005	0.008	0.115
		O_{3+4}	12	12	25	16	0.005	0.006	0.008	0.116
	BC	O_{3+4+7}	10	10	17	12	0.003	0.004	0.006	0.115
		O_{3+4}	10	10	21	14	0.005	0.006	0.007	0.115
<i>Yrt</i>	MP	O_{3+4+1}	11	11	28	14	0.009	0.031	0.035	0.327
		O_{3+4}	12	12	33	18	0.010	0.034	0.042	0.327
	BC	O_{3+4+7}	9	9	31	18	0.010	0.035	0.013	0.325
		O_{3+4}	12	12	35	21	0.010	0.035	0.041	0.326
<i>Atpa</i>	MP	O_{3+4+1}	9	4	6	6	0.001	0.003	0.005	0.204
		O_{3+4}	12	12	22	9	0.005	0.015	0.013	0.208
	BC	O_{3+4+7}	9	8	22	17	0.004	0.006	0.010	0.204
		O_{3+4}	12	11	27	16	0.005	0.016	0.019	0.209
<i>Fmr1</i>	MP	O_{3+4+1}	10	10	30	24	0.004	0.007	0.010	0.150
		O_{3+4}	11	11	38	25	0.005	0.009	0.012	0.151
	BC	O_{3+4+7}	8	7	19	12	0.003	0.006	0.007	0.150
		O_{3+4}	10	10	28	18	0.004	0.008	0.010	0.151

Table 1. Nucleotide variation and divergence per chromosomal arrangement for the six genes studied. *Pop*, population: Mt. Parnes (MP) and Barcelona (BC); *n*, sample size; *h*, number of haplotypes; *S*, number of polymorphic sites; π , nucleotide diversity in all sites; π_{sil} , nucleotide diversity in synonymous sites and non-coding positions; θ_{sil} , heterozygosity in silent sites; K_{sil} , divergence per silent site between *D. subobscura* and *D. pseudoobscura*.

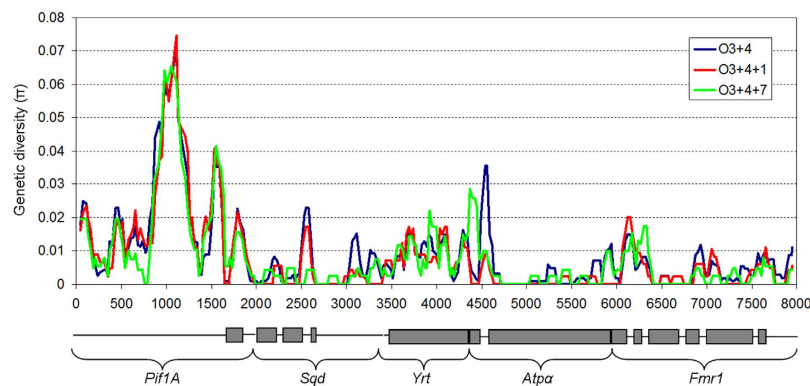


Figure 2. Genetic diversity (π) for the O_{3+4} , O_{3+4+1} and O_{3+4+7} chromosomal arrangements using the concatenated genes data set. Grey boxes and solid lines underneath mark exonic and intronic regions, respectively.

and O_{3+4+7} sequences alone, than compared to the O_{3+4} arrangement, suggesting the presence of recombination events between arrangements.

The low levels of linkage disequilibrium detected within inverted regions suggest that recombination between chromosomal arrangements may be frequent. Recombination was detected within and between arrangements for all genes (Rho, Table S1). Surprisingly, recombination estimates were higher when comparing different chromosomal arrangements than when comparing the same inversion. This result may simply be due to the higher number of informative sites when combining arrangements. Some gene conversion tracts (GCTs) were detected (Table S2) despite probabilities of a site to be informative for gene conversion events (ψ values) are low (10^{-3} to 10^{-4}). A total of five and eight tracts were observed between O_{3+4} - O_{3+4+1} and O_{3+4} - O_{3+4+7} , respectively. The lengths of the tracts were highly variable, ranging from 7 to 1573 bp, and the largest tracts were found in the *Atpa*

	$O_{3+4} - O_{3+4+1}$	$O_{3+4} - O_{3+4+7}$	$O_{3+4+1} - O_{3+4+7}$
<i>Pif1A</i>	-0.028 ns	0.146**	0.076 ns
<i>Abi</i>	-	0.065*	-
<i>Sqd</i>	0.082*	0.040*	0.071**
<i>Yrt</i>	0.017 ns	-0.001 ns	0.024 ns
<i>Atpα</i>	0.614***	0.525**	0.367***
<i>Fmr1</i>	-0.033 ns	0.004 ns	-0.005 ns
Concatenated	0.099*	0.182**	0.092*

Table 2. F_{ST} values for each gene and the concatenated set and the statistical significance of Snn (ns, not significant; $0.01 < *P < 0.05$; $0.001 < **P < 0.01$; $***P < 0.001$). Genes in grey are located inside inversions.

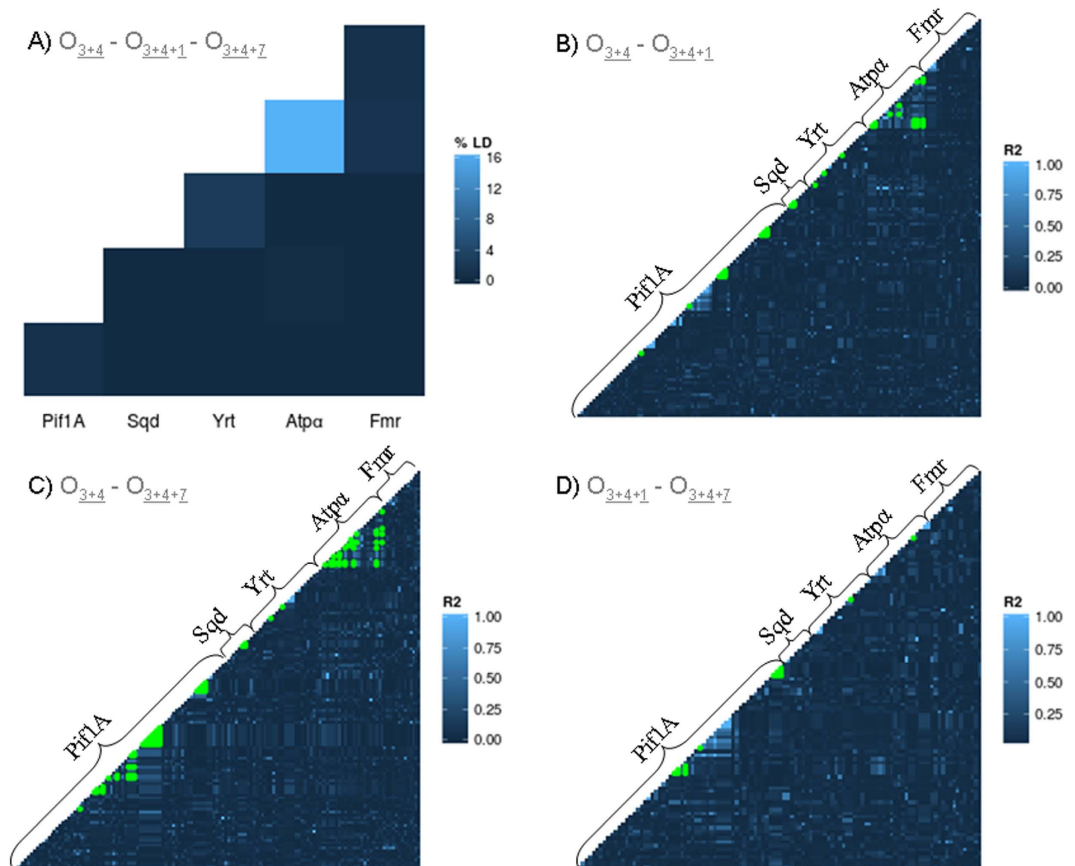


Figure 3. (A) Percentage of significant LD among O_{3+4} , O_{3+4+1} and O_{3+4+7} arrangements within and between genes. (B–D) Pairwise LD measured as R^2 for $O_{3+4+7} - O_{3+4}$, $O_{3+4+1} - O_{3+4}$ and $O_{3+4+1} - O_{3+4+7}$ comparisons. Green dots correspond to the significant associations after adjusting for multiple comparisons using Benjamini and Hochberg method (1995). Gene order in O_{3+4} and O_{3+4+1} is the same (Fig. 1) and has been used for homogeneity in all comparisons.

gene. Since GCTs are expected to be small, the large tracts observed might be due to single or double crossover events, given that *Atpα* gene is located outside the inversion.

Sequence networks for all genes were highly reticulated, with the exception of the *Atpα* gene, suggesting high levels of recombination among individuals carrying different chromosomal arrangements for genes located inside and outside inversions (Suppl. Fig. 2). For the *Sqd* gene, despite being located within all three inversions and presenting significant F_{ST} values between arrangements (Table 2), individual sequences of the same arrangement seldom clustered together suggesting high rates of exchange among chromosomal arrangements (Suppl. Fig. 2). For the *Atpα* gene, it was possible to distinguish three clades corresponding to each arrangement, although four recombinant individuals (FMP2, FBC49, FBC76 and MP36) could be identified matching those detected as GCT (Table S3). Two of them have the O_{3+4} arrangement (FMP2 and FBC49) and a GCT length larger than 1422 bp (Table S2), FBC76 has the O_{3+4+7} arrangement and also a large GCT (1573bp) and MP36 has the O_{3+4+1} arrangement and a small GCT (52 bp). In addition, for the *Atpα* gene, the number of recombination connections within

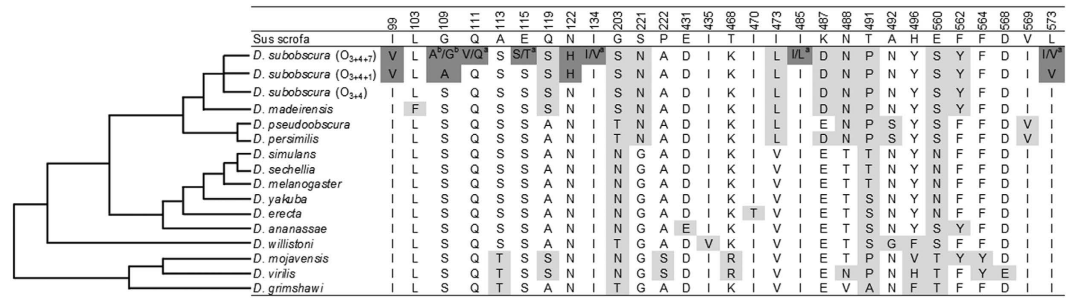


Figure 4. Amino acid replacements detected in the amplified region of the *Atpα* gene in 14 *Drosophila* species. ^alow frequency amino acid (<0.3); ^bequal frequency amino acid. Numbering corresponds to the mature pig enzyme (GenBank #: 1 × 03938). Shading is as follows: Pale grey: amino acid changes that occurred in the O_{3+4} arrangement of *D. subobscura* or in any other *Drosophila* species. Dark grey: changes found only in the O_{3+4+1} and/or O_{3+4+7} arrangements in comparison to the other *Drosophila* species.

O_{3+4+1} and O_{3+4+7} arrangements was lower than within the O_{3+4} arrangement (Suppl. Fig. 2), which could indicate a more recent origin of the former two arrangements.

Inversion ages may be overestimated from genes located in central positions of inverted regions, since they are more prone to be included in double crossovers consequently introducing additional variation from other arrangements. We estimated the age of the O_{3+4+7} arrangement using the *Sqd* gene, which is the closest to the proximal breakpoint of the O_7 inversion (Fig. 1), to be 0.47 ± 0.12 Myr assuming that the divergence time between *D. subobscura* and *D. pseudoobscura* is 17.7 ± 4.4 Myr¹⁹. The age of the O_{3+4+1} arrangement was estimated to be 0.52 ± 0.13 Myr using the *Sqd* gene and the same divergence time. BEAST program could not be used to estimate the age of those two inversions due to the high recombination detected among the three arrangements (Suppl. Fig. 2).

Test of neutrality and adaptive evolution. To evaluate whether any of the six genes are under positive selection, we performed several statistical tests for departure from the expectations of an equilibrium neutral model of evolution. A majority (93%) of the Tajima's D and Fu and Li's D test statistics were negative (Table S4). These overall results suggest a general trend towards an excess of low frequency polymorphisms that could be due to population growth. It is worth noting that Tajima's D and Fu and Li's D test were only significant for the *Atpα* gene in the O_{3+4+1} arrangement when using all positions (Table S4), although both tests failed to detect significant departures from neutrality when excluding the recombinant individual MP36 and/or using only silent sites (Table S5). In contrast, Tajima's D test was statistically significant for *Atpα* in the O_{3+4+7} arrangement when excluding recombinant individuals but not when using silent sites only (Table S5), raising the possibility of negative selection on polymorphic amino acid replacements at this gene.

The McDonald and Kreitman test, which contrasts nonsynonymous and synonymous polymorphism and divergence, was only significant for the *Atpα* gene in the O_{3+4+7} arrangement ($P = 0.0003$). For this gene, the number of polymorphic sites was 9 (7 nonsynonymous and 2 synonymous), while the number of differences between species was 60 (9 nonsynonymous and 51 synonymous, Table S6, Supporting information). The Direction of Selection (DoS) statistic is -0.442 for the O_{3+4+7} arrangement of this gene (Table S6, Supporting information). If one assumes synonymous sites are neutral, then this pattern would indicate an excess of nonsynonymous polymorphism present at the *Atpα* gene within the O_{3+4+7} arrangement. Certain amino acid changes nearly fixed in this arrangement (99, 109, 111 and 122 probably implicated in resistance to plant toxins, see below) could be maintained by diversifying selection as polymorphisms, while the rest are low frequency variants that could be weakly deleterious and kept at low frequencies by negative selection.

We tested for long-term positive selection at the *Atpα* gene using several site and branch-site tests implemented in CodeML of the PAML v4 package²⁰, that were based on the consensus sequences of the arrangements (see methods). All positions in the consensus sequences correspond to nearly fixed substitutions between lineages except for amino acid position 109 in the O_{3+4+7} arrangement (Fig. 4) where the two equally likely substitutions (A/G) were evaluated separately. Site tests of the entire gene fragment (M1a vs M2a and M7 vs M8, see Materials and Methods section), which assume that the strength and direction of selection is uniform across all lineages, failed to detect positively selected sites in the *Atpα* gene (Table S7). However, the branch-site test 2, that allows to detect sites that evolved under positive selection in a specific lineage, inferred positive selection for several codons on the O_{3+4+7} arrangement regardless of which amino acid is present in position 109 (Table S7), but not on the O_{3+4} and O_{3+4+1} arrangements. Positions that showed departures from neutrality according to PAML in the O_{3+4+7} arrangement are 99, 109, 111 and 122, which are the positions highlighted in the structural protein model (Fig. 5). In fact, positions 111 and 122 are the ones affecting the ouabain-*Atpα* interaction (see below), and the nonsynonymous change at position 111 was only found in O_{3+4+7} . Using BEAST, after removing recombinants, the time to most recent common ancestor (TMRCA) was estimated in 0.21 ± 0.009 Myr (mean \pm SE) for O_{3+4+1} , 0.46 ± 0.018 Myr for O_{3+4+7} and 1.69 ± 0.05 Myr for all O_{3+4} . Using the average silent nucleotide diversity the time to most recent common ancestor (TMRCA) was estimated in 0.09 ± 0.02 Myr and 0.13 ± 0.03 Myr for O_{3+4+1} and O_{3+4+7} respectively considering that the divergence time between *D. subobscura* and *D. pseudoobscura* is 17.7 ± 4.4 Myr¹⁹.

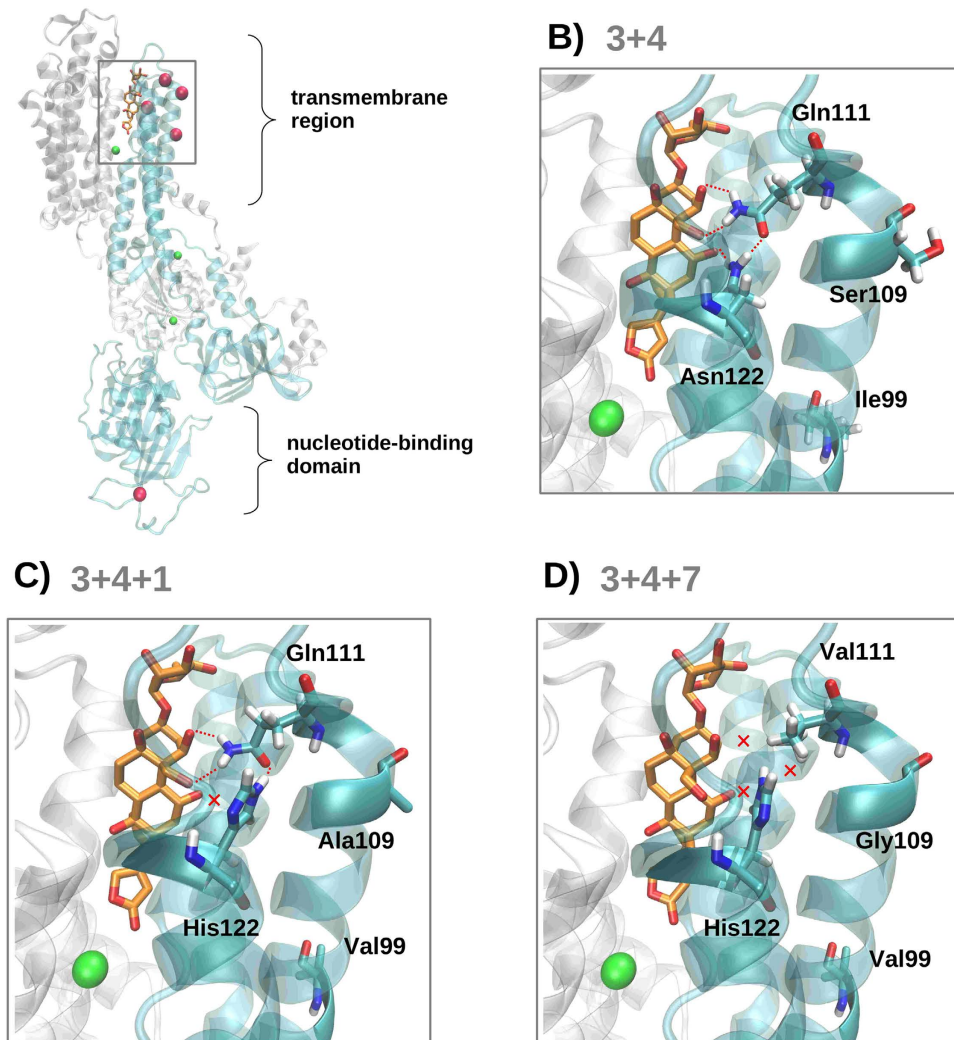


Figure 5. (A) Structural model of the ATPase α -subunit. The gene region sequenced is depicted in cyan and ouabain in orange sticks. Pink spheres represent positions presenting variation between arrangements and green spheres show the ion positions derived from the crystal structure of the template. (B–D) Detailed view of mutations located in the transmembrane region of O_{3+4} , O_{3+4+1} and O_{3+4+7} arrangements. Hydrogen bonding interactions are represented as red dotted lines, while lack of these interactions is signalled with a red cross.

We checked whether the variability in the *Atp α* gene, and specifically the nonsynonymous changes, were already present in other drosophilids or appeared *de novo* in *D. subobscura*. Amino acid replacements observed within the amplified region of the *Atp α* gene among 14 *Drosophila* species are summarized in Fig. 4. Most of the replacements detected can be assigned to specific lineages. For instance, a G to N replacement at position 221 and V to L replacement at position 473 were both detected for all species of the *obscura* group. Interestingly, some changes were only detected in O_{3+4+1} and O_{3+4+7} arrangements and not in any other of the thirteen drosophilids studied neither in the O_{3+4} arrangement of *D. subobscura*. These changes can be classified in three groups: shared mutations between the two arrangements (positions 99, 109 and 122), specific high frequency mutations in one arrangement (position 111 for O_{3+4+7} and 573 for O_{3+4+1}), and specific low frequency mutations (115, 134, 485, 573 for the O_{3+4+7}). The two equally frequent polymorphic amino acids in position 109 of the O_{3+4+7} arrangement (A and G) are small and non-polar, while the ancestral amino acid was polar (S) (Fig. 4). The O_{3+4} arrangement of *D. subobscura* is more similar to (closely) related species (i.e. *D. madeirensis*) than to O_{3+4+1} and O_{3+4+7} arrangements.

Three-dimensional structure of the ATPase α -subunit and putative functional consequences.

At least two of the amino acid replacements observed in the ATPase α -subunit may impact the binding of the cardenolide ouabain, a plant toxin capable of blocking ATPases^{21,22}. According to the crystallized ouabain–Na⁺, K⁺–ATPase complex²³, ouabain would interact with a set of hydrophobic residues in helices α M4 and α M5 and would establish particular polar interactions with helices α M1, α M2 and α M6. Helices α M1, α M2 were sequenced in the present work and are depicted in cyan in Fig. 5. The positions contributing to variation between arrangements are located both in the transmembrane region of the protein as well as in its nucleotide-binding domain (depicted

as magenta spheres in Fig. 5A). Of the variants located in the transmembrane region, we can expect different levels of impact regarding ouabain binding. Changes in positions 99 and 573 (I99V and I573V), which are located in the transmembrane and nucleotide-binding domain respectively, are similar in terms of hydrophobicity and shape and are not expected to have a big impact in terms of protein function. In the case of amino acid position 109 of the transmembrane segment, amino acid replacement results in a loss of a polar residue that could indirectly affect protein stability and insertion in the lipid bilayer (S109A in O_{3+4+1} and S109A, G in the O_{3+4+7} arrangement, Fig. 5B–D). Interestingly, we detected two further changes in the transmembrane region that could directly affect the binding of ouabain to the $Atp\alpha$ protein. In the O_{3+4} arrangement, ouabain establishes stabilizing hydrogen bonding interactions with residues Gln111 and Asn122 of the alpha subunit of the ATPase (Fig. 5B, red dashed lines). These interactions are further stabilized by a hydrogen bond between these two residues. In contrast, the replacement of Asn122 by His122 in both O_{3+4+1} and O_{3+4+7} arrangements destroys the interaction between this residue and ouabain (Fig. 5C, see red cross). In addition, mutation from Gln111 to Val111 in the O_{3+4+7} arrangement destroys the second stabilizing interaction as well as the intramolecular hydrogen bond formed by $Atp\alpha$ residues (Fig. 5D, see red crosses).

Discussion

Chromosomal inversions are known to strongly influence patterns of genetic diversity within their breakpoints. The degree of inversion variability and differentiation depends on the time since the formation of the inversion, on its size (large inversions are more likely to have double-crossovers within them), and on selection pressure^{4,24–26}. Genetic differentiation for O_{3+4+1} and O_{3+4+7} arrangements was significant despite variability levels for most of the genes located within them seem to have recovered to the level observed in the O_{3+4} ancestral arrangement. We estimated the age of these derived inversions considering that the *Sqd* gene is roughly 0.50 Myr (assuming that the divergence time between *D. subobscura* and *D. pseudoobscura* is 17.7 ± 4.4 Myr)¹⁹. The age of the O_{3+4} arrangement was estimated to be 0.90 Myr using the same divergence time as mentioned above¹¹. Thus, as expected, the O_{3+4+1} and O_{3+4+7} arrangements are younger than O_{3+4} from which they most likely derived (Fig. 1). However, the *Sqd* gene network showed recombination connections between different arrangements, further preventing estimating inversion ages using the coalescent process, which may result in an overestimation of their age. It is worth noting that the estimation of inversion ages may vary between markers^{9,11,27,28}. Thus, our results should be interpreted with caution until more markers are available to confirm them.

The genetic differentiation that we found between $O_{3+4+1}-O_{3+4}$ and $O_{3+4+7}-O_{3+4}$ arrangements was smaller than between the older $O_{3+4}-O_{ST}$ arrangements^{9,11,27}. The presence of two overlapped inversions (O_3 and O_4) in the later comparison may prevent crossovers formation more efficiently due to physical constraints. Overlapped inversions may be an important non-selective factor modulating nucleotide variability patterns and their absence may facilitate recombination. The small F_{ST} values obtained for individual genes located within O_1 and O_7 inverted regions suggest the presence of frequent genetic exchange with non-inverted arrangements for these regions, supporting recombination as the main contributor to variability recovery²⁴.

We did not detect a significant relationship between genetic variability and distance to breakpoints, as observed in previous studies of *D. subobscura*^{9,10}, *D. buzzatti*²⁹, and *Anopheles gambiae*³⁰. However, for *D. melanogaster* mixed results are obtained depending on the inversions and populations of origin evaluated, with peaks of high and low variability and differentiation interspersed^{31,32}. We find that genetic differentiation close to inversion breakpoints can also be eroded through time at a gene specific rate, supporting previous experimental studies in *D. subobscura*¹⁵, and contrasting with those obtained in *D. pseudoobscura*³³. As expected by the presence of high levels of recombination, linkage disequilibrium levels were low within inversions. Our results contrast with those obtained in *D. pseudoobscura* inversions, which generally show high levels of LD between genes associated with inversions that have been interpreted as an evidence for epistasis^{6,34}. For *D. melanogaster* strong LD within the region spanned by In(3R)Payne has been detected although it is not uniformly distributed³¹. According to tests of neutrality based on frequency distributions (Tajima's D and Fay and Wu's H), there was a tendency towards an excess of low frequency polymorphisms for all genes consistent with a recent expansion of the species³⁵, but only the *Atp\alpha* gene departed from neutral expectations. Taken altogether, variability in all genes (with the only exception of the *Atp\alpha* gene) in the O_{3+4+1} and O_{3+4+7} arrangements seem to be shaped mainly by extensive recombination rather than Darwinian (positive) selection.

Our results indicate that variability patterns of the *Atp\alpha* gene seem to be strongly influenced by natural selection in the O_{3+4+1} and the O_{3+4+7} arrangements. Despite being located outside both studied inversions (but less than 2 Mb apart from the closest inversion breakpoint), we detected high levels of genetic differentiation when compared to the ancestral O_{3+4} arrangement due to fixed nonsynonymous differences. In *D. melanogaster* parallel geographic variation in regions inside and outside inversions have been observed across continents³⁶. Besides that, SNPs varying in frequency seasonally throughout *D. melanogaster* genome—and not exclusively concentrated in inversions—have also been described³⁷. Thus, spatial and temporal varying selection seems also to strongly influence regions outside inversions. Differences in the *Atp\alpha* gene between O_{3+4+1} and O_{3+4+7} arrangements were significant at the nucleotide level although at the amino acid level, both arrangements are nearly identical. Interestingly, all specific changes of the *D. subobscura* lineage occurred in the O_{3+4+1} and/or O_{3+4+7} arrangements, since changes detected in the O_{3+4} arrangement were shared with *D. madeirensis*, which is consistent with their common ancestry. In addition, protein sequences of O_{3+4} and O_{ST} arrangements of *D. subobscura* were reported to be identical¹¹.

The nature of natural selection acting on the *Atp\alpha* gene is quite complex. The McDonald-Kreitman test was significant for *Atp\alpha* gene and the Direction of Selection (DoS) statistic was negative in a direction consistent with strong selective constraint acting on most of the protein. These results are in agreement with the essential nature of this gene for individual survival. Nonetheless, PAML did reveal significant evidence for positive selection acting on several codons within the *Atp\alpha* gene, including amino acid replacements at two codons that would confer

resistance to a plant toxin. Positive selection acting on highly conserved genes has also been reported in other studies: according to Pupko & Galtier³⁸, primate mitochondrial genomes evolved through episodes of positive selection at a few sites, enabling the fine-tuning of the three-dimensional protein structure to optimize the function of conserved genes. Similarly, Vasseur *et al.*³⁹ found rare alleles with evidence of positive selection in some genes of the NLR family although this family is under strong purifying selection due to its vital role.

The case of the *Atpα* gene indicates that positive selection is able to act within a highly conserved gene to maintain adaptive mutations associated with certain chromosomal inversions. The structural analysis of the ouabain-ATPase α -subunit complex shows that two substitutions, both in the O_{3+4+1} and the O_{3+4+7} arrangements (111V and 122H), would reduce the affinity of the ATPase complex to bind the cardenolide ouabain due to the destruction of stabilizing hydrogen bonds. Remarkably, these observations are in line with mutagenesis studies showing a significantly increased survival of cells transfected with constructs having mutations 111V and 122H (from *D. melanogaster*) after ouabain treatment, and a 2.250-fold increased resistance to this toxin when bearing both mutations^{21,40}. Previous studies demonstrated that adaptive mutations in Na,K-ATPase, such the ones in positions 111 and 122, were acquired in parallel in some cardenolide-feeding species^{21,22}. Three hypotheses could explain the presence of convergent mutations in O_{3+4+1} and O_{3+4+7} arrangements in *D. subobscura*. (1) In a parallel scenario⁴¹, mutations may have occurred independently in the two new arrangements as the result of adaptation to similar environmental conditions. (2) In a collateral scenario⁴¹, variants from an ancestral polymorphism could have been independently captured during the formation of the two inversions and subsequently been maintained by selection. (3) Finally, amino acid substitutions that occurred in one of the two arrangements in response to selection could have been subsequently acquired by the other inversion through double recombination or gene conversion between arrangements, with those variants being subsequently driven to high frequency in both arrangements due to similar selective pressures. All three of these possible scenarios include natural selection and suggest that epistatic interactions between the *ATPα* gene and genes located inside both inversions (O_1 and O_7) are necessary to account for the maintenance of amino acid similarities despite *ATPα* gene being located outside both inversions. Furthermore the reduced number of recombinants with O_{3+4} can only be explained by selection if recombinant individuals are effectively purged from populations to maintain adaptive interactions. Currently available data does not allow us to discriminate between these three scenarios although the collateral hypothesis seems less likely since in *D. madeirensis*, O_{3+4} and O_{ST} share almost identical amino acid composition. Given the high chromosomal polymorphism in *D. subobscura* and the many inversion breakpoints in the neighbouring area of the *Atpα* gene⁸, future analysis of other chromosomal arrangements may help to reconstruct the process of acquisition of these adaptive substitutions, and to determine whether they were already present in a common ancestor (i.e. synapomorphy) or acquired by parallel evolution or through recombination.

Cardenolides have a huge diversity of chemical forms and are sporadically distributed across 12 families of angiosperms⁴². Cardenolide feeding species have been typically associated with plants of the family Apocynaceae, notably in the genera *Asclepias* and *Apocynum*^{21,22}. *Asclepias* has a Nearctic distribution and *Apocynum* a temperate Northern hemisphere distribution⁴³, and cardenolides production seems to form latitudinal clines of different sign depending on the *Asclepias* species^{42,44}. *D. subobscura* is a generalist saprophytic insect and its diet includes decaying plant material and fruits, fungi, yeast and microbials⁴⁵, and it is known to be able to feed from decaying *Digitalis purpurea*⁴⁶, a plant containing ouabain. We hypothesize that the appearance of mutations in the O_{3+4+7} and O_{3+4+1} arrangements conferring the ability to feed on cardenolide containing plants has changed the fitness of associated chromosomal inversions resulting in nonsynonymous polymorphism. Thus, in certain environments (i. e. in the presence of toxic plants) positive selection will favour the maintenance of adaptive variants. Future studies may help elucidate whether the observation of adaptive mutations in some arrangements of *D. subobscura* reflects geographical distribution of cardenolide-containing plants in the Mediterranean region and confirm whether these amino acid substitutions confer resistance to cardenolides in these insects.

Materials and Methods

Fly samples and DNA sequencing. A total of 45 isochromosomal lines for the O chromosome of *D. subobscura* derived in Araúz *et al.*¹⁸ were used: 11 O_{3+4+1} and 12 O_{3+4} lines from Mt. Parnes (Greece) and 10 O_{3+4+7} and 12 O_{3+4} lines from Barcelona (Spain). Genes were selected according to their chromosomal location within or nearby the studied inversions (Fig. 1). The six genes are *Pif1A* (PFTAIRE-interacting factor 1A), *Abi* (Abelson interacting protein), *Sqd* (Squid), *Yrt* (Yurt), *Atpα* (Na pump α subunit) and *Fmr1* (Fragile X mental retardation). Genomic DNA extraction, DNA amplification and sequencing reactions for the O_{3+4+1} and O_{3+4+7} arrangements were carried out as reported in Pegueroles *et al.*¹¹. Sequencing was done on a 3730 Analyzer (Applied Biosystems) at the Serveis Científic-Tècnics from Universitat de Barcelona. Sequences were assembled with SeqMan II (DNASTAR) and multiply aligned with Clustal W⁴⁷ implemented in BioEdit v7⁴⁸. Sequences for the O_{3+4+7} and O_{3+4+1} arrangements are available at GenBank under the accession numbers KT318937- KT319043. Sequences for the O_{3+4} arrangement of *D. subobscura* and *D. madeirensis* were obtained from GenBank (accession # JN882382-JN882400, JN882406-JN882429, JN882441-JN882461, JN882472-JN882495, JN882508-JN882529, JN882541- JN882564 and JN882376-JN882381). Sequences from the other 12 *Drosophila* species with sequenced genome were downloaded from Flybase database (<http://flybase.org>).

Nucleotide polymorphism and genetic differentiation. Nucleotide polymorphism and genetic differentiation were estimated with DnaSP v5⁴⁹. We calculated the standard parameters of molecular diversity: number of haplotypes (*h*), number of polymorphic sites (*S*) and number of singletons, nucleotide diversity (π)⁵⁰, nucleotide diversity in synonymous sites and non-coding positions (π_{sil})⁵¹, silent site heterozygosity (θ_{sil})⁵² and divergence per silent site between *D. subobscura* and *D. pseudoobscura* (K_{sil})⁵¹. Due to the presence of duplications in the *Abi* gene (data not shown), very few individuals could be sequenced for the O_{3+4+1} arrangement. Thus, the concatenated data set does not contain *Abi* gene sequences. Overall, 21 O_{3+4} , 10 O_{3+4+1} and 8

O_{3+4+7} chromosomes were included in the concatenated data set and genes combined with Concatenator v1⁵³. Nucleotide diversity (π) across the concatenated data was calculated using a sliding window of 100 nucleotides with a step size of 25. Genetic distances were computed with F_{ST} ⁵⁴ and Snn⁵⁵ and its significance estimated with 10,000 replicates. The distance of each gene to the nearest inversion breakpoint in bp was calculated assuming that all cytological bands contain the same genetic content and the length of the O chromosome of *D. subobscura*, but not its gene order⁵⁶, is equivalent to that of the chromosome 2 of *D. pseudoobscura* as in Pegueroles *et al.*⁵⁷.

Neutrality tests. Tajima's D ⁵⁸ and Fu and Li's D ⁵⁹ tests were carried out to assess whether the site frequency spectrum of variation within arrangements differ from their expectation under an equilibrium neutral model, using *D. pseudoobscura* as an outgroup. This species was used as outgroup instead of *D. madeirensis* since the level of divergence to *D. subobscura* for the latter is too low for these genes¹¹. Furthermore, to test for footprints of selection we performed the McDonald and Kreitman⁶⁰ test, the Direction of Selection (DoS) statistic⁶¹, and several site and branch-site tests implemented in CodeML of the PAML v4 package²⁰. Site tests of the entire gene, allowing the ω ratio to vary among sites, were performed comparing two pairs of models, the nearly neutral model M1a (model = 0; NSsites = 1) with the alternative positive selection model M2a (model = 0; NSsites = 2), and the neutral model M7 (model = 0; NSsites = 7, ncatG = 10) with the alternative selection model M8 (model = 0; NSsites = 8, ncatG = 10). For the branch-site test 2, aiming to detect positive selection affecting a few sites, in the neutral model we used the parameters model = 2, NSsites = 2, fix_omega = 1 and omega = 1. and for the alternative selection model we used model = 2, NSsites = 2, fix_omega = 0 and omega = 1.5. All these tests were applied to the *Atp α* gene after excluding recombinant individuals and using the consensus sequences of the O_{3+4} , O_{3+4+1} and O_{3+4+7} arrangements of *D. subobscura* with both *D. madeirensis* and *D. pseudoobscura* sequences as outgroups. Neutral and alternative models were compared using a likelihood ratio test and the P-value was assessed using a chi-squared test.

Linkage disequilibrium and recombination. For the concatenated data set we estimated the percentage of pairwise comparisons between informative sites presenting significant linkage disequilibrium (LD), and their statistical significance was analysed with Fisher's exact test implemented in DnaSP v5⁵⁰. P-values were adjusted for multiple testing using the false discovery rate method of Benjamini & Hochberg⁶². LD between pairs of polymorphic sites was also measured with r^2 parameter⁶³ and Z_{IS} ⁶⁴ as a global measure of LD obtained with DnaSP. LD plots were performed using ggplot2 package⁶⁵. The population recombination rate ($\rho = 4N_e r$, where N_e is the effective population size and r is the rate of recombination) was estimated using a composite likelihood method⁶⁶ computed with LDhat v2.1 (<http://www.stats.ox.ac.uk/~mcvean/LDhat/instructions.html>). Recombination networks were constructed using SplitsTree4 program⁶⁷. Gene conversion tracts (GCT) were identified using the method of Betrán *et al.*⁶⁸ implemented in DnaSP. In order to avoid confounding effects due to the population of origin, F_{ST} , ρ , GCT and LD parameters were calculated between arrangements from the same population, despite the lack of genetic differentiation observed between O_{3+4} arrangements from different populations¹¹.

Age of inversions. The ages of inversions were estimated for the *Sqd* gene, since it is located inside the inverted regions and close to the breakpoint (Fig. 1), using the average silent nucleotide diversity within inversions and excluding individuals carrying gene conversion tracts^{10,11,27}. The number of substitutions per site per year was calculated using the divergence per silent site between *D. subobscura* and *D. pseudoobscura*, based on our sequences and using divergence time of 17.7 ± 4.4 Myr¹⁹. We dated the time to the most recent ancestor (TMRCA) for the O_{3+4+1} and O_{3+4+7} arrangements of the *Atp α* gene using the same method and also using BEAST 1.8.0⁶⁹. We used a lognormal relaxed clock model and considered the same divergence time and a mutation rate of 0.011 estimated for *Drosophila* species based on 176 nuclear genes¹⁹. The substitution model used was HKY + G + I, being the best substitution model for the *Atp α* gene inferred with jModelTest 2.0^{70,71}, with runs of 2 million steps, sampling a tree every 200 steps. Tracer v1.6⁷² was used to check convergence of parameters and to obtain mean and standard errors (SE) of the time to the most common ancestor of all sequences for a given inversion. We discarded 10% of the steps as burn-in. In both methods we did not include recombinant individuals MP36 and FBC76.

Structural analysis of the Na⁺,K⁺-ATPase–ouabain complex. The crystal structure of a high-affinity Na⁺,K⁺-ATPase–ouabain complex (PDB ID 4HYT), which shows a 74% amino acid sequence identity with the predicted ATP α protein for *D. subobscura*, was selected for homology modelling. The model was built using the MOE package (<http://www.chemcomp.com/software.htm>). After sequence alignment (default settings), ten models were generated using the Amber12:EHT force field⁷³. The best model for each arrangement was selected and superposed on the PDB ID 4HYT crystal structure in order to align the cardenolide ouabain, a plant toxin capable of blocking ATPases, to the newly obtained homology models. The resulting ouabain-receptor complexes were further refined by performing an energy minimization of ouabain and its binding pocket (defined as all residues at 4.5 Å of the compound) using the Amber12:EHT force field by applying gradient minimization until the RMS gradient was lower than 0.001 kcal mol⁻¹ Å⁻¹. Representations of ouabain-receptor complexes were created using VMD 1.9.1⁷⁴.

References

- Kawecki, T. J. & Ebert, D. Conceptual issues in local adaptation. *Ecol. Lett.* **7**, 1225–1241 (2004).
- Savolainen, O., Lascoux, M. & Merilä, J. Ecological genomics of local adaptation. *Nat. Rev. Genet.* **14**, 807–820 (2013).
- Prevosti, A. *et al.* Colonization of America by *Drosophila subobscura*: Experiment in natural populations that supports the adaptive role of chromosomal inversion polymorphism. *Proc. Natl. Acad. Sci. USA* **85**, 5597–5600 (1988).
- Hoffmann, A. A. & Rieseberg, L. H. Revisiting the impact of inversions in evolution: from population genetic markers to drivers of adaptive shifts and speciation? *Annu. Rev. Ecol. Evol. Syst.* **39**, 21–42 (2008).

5. Kapun, M., van Schalkwyk, H., McAllister, B., Flatt, T. & Schlötterer, C. Inference of chromosomal inversion dynamics from Pool-Seq data in natural and laboratory populations of *Drosophila melanogaster*. *Mol. Ecol.* **23**, 1813–1827 (2013).
6. Schaeffer, S. W. *et al.* Evolutionary genomics of inversions in *Drosophila pseudoobscura*: Evidence for epistasis. *Proc. Natl. Acad. Sci. USA* **100**, 8319–8324 (2003).
7. Balanyà, J. *et al.* Evolutionary pace of chromosomal polymorphism in colonizing populations of *Drosophila subobscura*: an evolutionary time series. *Evolution* **57**, 1837–1845 (2003).
8. Krimbas, C. B. *Drosophila subobscura: Biology, Genetics and Inversion polymorphism*. Verlag Dr. Kovac, Hamburg, Germany (1993).
9. Munté, A., Rozas, J., Aguadé, M. & Segarra, C. Chromosomal inversion polymorphism leads to extensive genetic structure: a multilocus survey in *Drosophila subobscura*. *Genetics* **169**, 1573–1581 (2005).
10. Nóbrega, C., Khadem, M., Aguadé, M. & Segarra, C. Genetic exchange versus genetic differentiation in a medium-sized inversion of *Drosophila*: the A2/AST arrangements of *Drosophila subobscura*. *Mol. Biol. Evol.* **25**, 1534–1543 (2008).
11. Pegueroles, C., Aquadro, C. F., Mestres, F. & Pascual, M. Gene flow and gene flux shape evolutionary patterns of variation in *Drosophila subobscura*. *Heredity* **110**, 520–9 (2013).
12. Rozas, J. & Aguadé, M. Gene conversion is involved in the transfer of genetic information between naturally occurring inversions of *Drosophila*. *Proc. Natl. Acad. Sci. USA* **91**, 11517–11521 (1994).
13. Navarro-Sabaté, A., Aguadé, M. & Segarra, C. Excess of nonsynonymous polymorphism at *Acp1* in different gene arrangements of *Drosophila subobscura*. *Mol. Biol. Evol.* **20**, 1833–1843 (2003).
14. Rodríguez-Trelles, F., Tarrío, R. & Santos, M. Genome-wide evolutionary response to a heat wave in *Drosophila*. *Biol. Lett.* **9**, 20130228 (2013).
15. Pegueroles, C., Ordóñez, V., Mestres, F. & Pascual, M. Recombination and selection in the maintenance of the adaptive value of inversions. *J. Evol. Biol.* **23**, 2709–2717 (2010).
16. Balanyà, J., Solé, E., Oller, J. M., Sperlich, D. & Serra, L. Long-term changes in the chromosomal inversion polymorphism of *Drosophila subobscura*. II. European populations. *J. Zool. Syst. Evol. Res.* **42**, 191–201 (2004).
17. Rodríguez-Trelles, F., Alvarez, G. & Zapata, C. Time series analysis of seasonal changes of the O inversion polymorphism of *Drosophila subobscura*. *Genetics* **142**, 179–187 (1996).
18. Araúz, P. A. *et al.* Tracking the origin of the American colonization by *Drosophila subobscura*: genetic comparison between Eastern and Western Mediterranean populations. *J. Zool. Syst. Evol. Res.* **47**, 25–34 (2009).
19. Tamura, K., Subramanian, S. & Kumar, S. Temporal patterns of fruit fly (*Drosophila*) evolution revealed by mutation clocks. *Mol. Biol. Evol.* **21**, 36–44 (2004).
20. Yang, Z. PAML 4: phylogenetic analysis by maximum likelihood. *Mol. Biol. Evol.* **24**, 1586–1591 (2007).
21. Dobler, S., Dalla, S., Wagschal, V. & Agrawal, A. Community-wide convergent evolution in insect adaptation to toxic cardenolides by substitutions in the Na,K-ATPase. *Proc. Natl. Acad. Sci. USA* **109**, 13040–13045 (2012).
22. Zhen, Y., Aardema, M. L., Medina, E. M., Schumer, M. & Andolfatto, P. Parallel molecular evolution in an herbivore community. *Science* **337**, 1634–1637 (2012).
23. Laursen, M., Yatime, L., Nissen, P. & Fedosova, N. U. Crystal structure of the high-affinity Na + K + -ATPase-ouabain complex with Mg²⁺ bound in the cation binding site. *Proc. Natl. Acad. Sci. USA* **110**, 10958–10963 (2013).
24. Navarro, A., Betran, E., Barbadilla, A. & Ruiz, A. Recombination and gene flux caused by gene conversion and crossing over in inversion heterokaryotypes. *Genetics* **146**, 695–709 (1997).
25. Dobzhansky, T. Genetics of natural populations. XIX. Origin of heterosis through natural selection in populations of *Drosophila pseudoobscura*. *Genetics* **35**, 288–302 (1950).
26. Powell, J. R. *Progress and prospects in Evolutionary Biology: The Drosophila model*. Oxford University Press, New York. (1997).
27. Rozas, J., Segarra, C., Ribó, G. & Aguadé, M. Molecular population genetics of the rp49 gene region in different chromosomal inversions of *Drosophila subobscura*. *Genetics* **151**, 189–202 (1999).
28. Navarro-Sabaté, A., Aguadé, M. & Segarra, C. The relationship between allozyme and chromosomal polymorphism inferred from nucleotide variation at the *Acp1* gene region of *Drosophila subobscura*. *Genetics* **153**, 871–889 (1999).
29. Laayouni, H., Hasson, E., Santos, M. & Fontdevila, A. The evolutionary history of *Drosophila buzzatii*. XXXV. Inversion polymorphism and nucleotide variability in different regions of the second chromosome. *Mol. Biol. Evol.* **20**, 931–944 (2003).
30. Cheng, C. *et al.* Ecological genomics of *Anopheles gambiae* along a latitudinal cline: a population-resequencing approach. *Genetics* **190**, 1417–1432 (2012).
31. Rane, R. V., Rako, L., Kapun, M., Lee, S. F. & Hoffmann, A. A. Genomic evidence for role of inversion 3RP of *Drosophila melanogaster* in facilitating climate change adaptation. *Mol. Ecol.* **24**, 2423–2432 (2015).
32. Daniel K. Fabian *et al.* Genome-wide patterns of latitudinal differentiation among populations of *Drosophila melanogaster* from North America. *Mol. Ecol.* **21**, 4748–4769 (2012).
33. Schaeffer, S. W. & Anderson, W. W. Mechanisms of genetic exchange within the chromosomal inversions of *Drosophila pseudoobscura*. *Genetics* **171**, 1729–1739 (2005).
34. Wallace, A. G., Detweiler, D. & Schaeffer, S. W. Molecular population genetics of inversion breakpoint regions in *Drosophila pseudoobscura*. *G3 (Bethesda)* **3**, 1151–63 (2013).
35. Pratdesaba, R., Segarra, C. & Aguadé, M. Inferring the demographic history of *Drosophila subobscura* from nucleotide variation at regions not affected by chromosomal inversions. *Mol. Ecol.* **24**, 1729–1741 (2015).
36. Reinhardt, J. A., Kolaczowski, B., Jones, C. D., Begun, D. J. & Kern, A. D. Parallel geographic variation in *Drosophila melanogaster*. *Genetics* **197**, 361–373 (2014).
37. Bergland, A. O., Behrman, E. L., Schmidt, P. S. & Petrov, D. A. Genomic evidence of rapid and stable adaptive oscillations over seasonal time scales in *Drosophila*. *Plos Genetics* **10**, e1004775 (2014).
38. Pupko, T. & Galtier, N. A covarion-based method for detecting molecular adaptation: application to the evolution of primate mitochondrial genomes. *Proc. Biol. Sci.* **269**, 1313–1316 (2002).
39. Vasseur, E. *et al.* The evolutionary landscape of cytosolic microbial sensors in humans. *Am. J. Hum. Genet.* **91**, 27–37 (2012).
40. Dalla, S., Swarts, H. G. P., Koenderink, J. B. & Dobler, S. Amino acid substitutions of Na,K-ATPase conferring decreased sensitivity to cardenolides in insects compared to mammals. *Insect Biochem. Mol. Biol.* **43**, 1109–1115 (2013).
41. Stern, D. L. The genetic causes of convergent evolution. *Nat. Rev. Genet.* **14**, 751–764 (2013).
42. Agrawal, A. A., Petschenka, G., Bingham, R. A., Weber, M. G. & Rasmann, S. Toxic cardenolides: chemical ecology and coevolution of specialized plant-herbivore interactions. *New Phytol.* **194**, 28–45 (2012).
43. Endress, M. E. & Bruyn, P. V. A revised classification of the Apocynaceae. *Bot. Rev.* **66**, 1–56 (2000).
44. Woods, E. C., Hastings, A. P., Turley, N. E., Heard, S. B. & Agrawal, A. A. Adaptive geographical clines in the growth and defense of a native plant. *Ecol. Monogr.* **82**, 149–168 (2012).
45. Markow, T. A. & O'Grady, P. Reproductive ecology of *Drosophila*. *Funct. Ecol.* **22**, 747–759 (2008).
46. Shorrock, B., Ashburner, M., Carson, H. L. & Thompson Jr, J. N. The breeding sites of temperate woodland *Drosophila*. In: *The genetics and biology of Drosophila*, pp. 385–428. Academic Press, London (1982).
47. Thompson, J. D., Higgins, D. G. & Gibson, T. J. CLUSTAL W: Improving the sensitivity of progressive multiple sequence alignment through sequence weighting, position-specific gap penalties and weight matrix choice. *Nucleic Acids Res.* **22**, 4673–4680 (1994).
48. Hall, T. A. BioEdit: a user-friendly biological sequence alignment editor and analysis program for Windows 95/98/NT. *Nucleic Acids Symp. Ser.* **41**, 95–98 (1999).

49. Librado, P. & Rozas, J. DnaSP v5: a software for comprehensive analysis of DNA polymorphism data. *Bioinformatics* **25**, 1451–1452 (2009).
50. Nei, M. *Molecular Evolutionary Genetics*. (Columbia University Press, New York, 1987).
51. Nei, M. & Gojori, T. Simple methods for estimating the numbers of synonymous and nonsynonymous nucleotide substitutions. *Mol. Biol. Evol.* **3**, 418–426 (1986).
52. Watterson, G. A. Number of segregating sites in genetic models without recombination. *Theor. Popul. Biol.* **7**, 256–276 (1975).
53. Pina-Martins, F. & Paulo, O. S. CONCATENATOR: Sequence data matrices handling made easy. *Mol. Ecol. Resour.* **8**, 1254–1255 (2008).
54. Hudson, R. R., Slatkin, M. & Maddison, W. P. Estimation of levels of gene flow from DNA-sequence data. *Genetics* **132**, 583–589 (1992).
55. Hudson, R. R. A new statistic for detecting genetic differentiation. *Genetics* **155**, 2011–2014 (2000).
56. Santos, J., Serra, L., Solé, E. & Pascual, M. FISH mapping of microsatellite loci from *Drosophila subobscura* and its comparison to related species. *Chrom. Res.* **18**, 213–226 (2010).
57. Pegueroles, C., Araúz, P. A., Pascual, M. & Mestres, F. A recombination survey using microsatellites: the O chromosome of *Drosophila subobscura*. *Genetica* **138**, 795–804 (2010).
58. Tajima, F. Statistical methods to test for nucleotide mutation hypothesis by DNA polymorphism. *Genetics* **123**, 585–595 (1989).
59. Fu, Y. X. & Li, W. H. Statistical tests of neutrality of mutations. *Genetics* **133**, 693–709 (1993).
60. McDonald, J. H. & Kreitman, M. Adaptive protein evolution at the *Adh* locus in *Drosophila*. *Nature* **351**, 652–654 (1991).
61. Stoletzki, N. & Eyre-Walker, A. Estimation of the neutrality index. *Mol. Biol. Evol.* **28**, 63–70 (2011).
62. Benjamini, Y. & Hochberg, Y. Controlling the false discovery rate: a practical and powerful approach to multiple testing. *J. R. Stat. Soc. Ser. B* **57**, 289–300 (1995).
63. Hill, W. G. & Robertson, A. Linkage disequilibrium in finite populations. *Theor. Appl. Genet.* **38**, 226–231 (1968).
64. Kelly, J. K. A test of neutrality based on interlocus associations. *Genetics* **146**, 1197–1206 (1997).
65. Wickham, H. *ggplot2: elegant graphics for data analysis*. Springer New York (2009).
66. Hudson, R. R. Two-locus sampling distributions and their application. *Genetics* **159**, 1805–1817 (2001).
67. Huson, D. H. & Bryant, D. Application of phylogenetic networks in evolutionary studies. *Mol. Biol. Evol.* **23**, 254–267 (2006).
68. Betrán, E., Rozas, J., Navarro, A. & Barbadilla, A. The estimation of the number and the length distribution of gene conversion tracts from population DNA sequence data. *Genetics* **146**, 89–99 (1997).
69. Drummond, A. J., Suchard, M. A., Xie, D. & Rambaut, A. Bayesian phylogenetics with BEAUti and the BEAST 1.7. *Mol. Biol. Evol.* **29**, 1969–1973 (2012).
70. Durrin, D., Taboada, G. L., Doallo, R. & Posada, D. jModelTest 2: more models, new heuristics and parallel computing. *Nature Methods* **9**, 772 (2012).
71. Guindon, S. & Gascuel, O. A simple, fast and accurate method to estimate large phylogenies by maximum-likelihood. *Systematic Biology* **52**, 696–704 (2003).
72. Rambaut, A., Suchard, M. A., Xie, D. & Drummond, A. J. *Tracer v1.6*. Available from <http://beast.bio.ed.ac.uk/Tracer> (2014).
73. Gerber, P. R. & Müller, K. MAB, a generally applicable molecular force field for structure modelling in medicinal chemistry. *J. Comput. Aided. Mol. Des.* **9**, 251–268 (1995).
74. Humphrey, W., Dalke, A. & Schulten, K. VMD: visual molecular dynamics. *J. Mol. Graph.* **14**, 33–38 (1996).

Acknowledgements

We thank Ferran Palero, Celia Schunter, Casandra Riera, Iain Patten, Carolyn Newey and the entire Aquadro's lab for their valuable comments on the manuscript. We also thank Pedro A. Araúz for the collection of the flies and his collaboration carrying out the genetic crosses, Joan Balanyà for the analyses of the polytene chromosomes and Gemma Calabria and Olga Dolgova for their collaboration in the *in situ* hybridizations. We are also grateful to two anonymous reviewers for helpful comments that improved the manuscript. This work was supported by a pre-doctoral fellowship to CP (2009FIC-00096) from the Generalitat de Catalunya (Spain). Research was funded by projects CGL2006-13423-C02-02 from the Ministerio de Ciencia y Tecnología (MCYT, Spain) and CTM2013-48163-C2-2-R from the Ministerio de Economía y Competitividad (MINECO, Spain). MP and FM are members of the research group 2014-SGR336 from the Generalitat de Catalunya (Spain).

Author Contributions

C.P., C.F.A., M.P. and F.M. designed the research; C.P., A.F.C., M.M.S. and M.P. performed the experimental work and analyses; C.P. wrote the first draft of the manuscript, and subsequently, all authors contributed to the writing.

Additional Information

Accession codes: D. subobscura sequences data are available at GenBank under the accessions numbers KT318937- KT319043.

Supplementary information accompanies this paper at <http://www.nature.com/srep>

Competing financial interests: The authors declare no competing financial interests.

How to cite this article: Pegueroles, C. *et al.* Inversions and adaptation to the plant toxin ouabain shape DNA sequence variation within and between chromosomal inversions of *Drosophila subobscura*. *Sci. Rep.* **6**, 23754; doi: 10.1038/srep23754 (2016).



This work is licensed under a Creative Commons Attribution 4.0 International License. The images or other third party material in this article are included in the article's Creative Commons license, unless indicated otherwise in the credit line; if the material is not included under the Creative Commons license, users will need to obtain permission from the license holder to reproduce the material. To view a copy of this license, visit <http://creativecommons.org/licenses/by/4.0/>